Separation and Purification Technology 221 (2019) 74–82

Contents lists available at ScienceDirect

Separation and Purification Technology

journal homepage: www.elsevier.com/locate/seppur

Enhancing gas separation efficiency by surface functionalization of nanoporous membranes

I.S. Sadilov[a], D.I. Petukhov[a,b,*], A.A. Eliseev[a,b]

[a] Department of Materials Science, Lomonosov Moscow State University, 1-73 Leninskiye gory, Moscow 11 9991, Russia
[b] Department of Chemistry, Lomonosov Moscow State University, 1-3 Leninskiye gory, Moscow 11 9991, Russia

ARTICLE INFO

Keywords:
Surface modification
TMAC
Adsorption
Hydrocarbon gases separation
Anodic alumina membranes

ABSTRACT

Here we report evidence for substantial changes in the separation efficiency of nanoporous anodic alumina membranes with nanochannel diameters ranging from 10–100 nm modified with octadecylphosphonic acid in the transitional flow regime. Softening of surface by alkyl groups with a surface density ~2 groups/nm^2 leads to a general permeance decrease in 3–500 times, depending strongly on the penetrant gas nature and the channels diameter. The divergence of the permeance, for different gases, increases with the decreasing diameter of the pores. For a surface-functionalized membrane, with 10-nm channel diameters, it results in n-C_4H_{10}/CH_4 ideal and mixed gas separation factors up to 32.3 and 9.0 respectively at a n-C_4H_{10} permeance up to 3.5 m^3/(m^2·bar·h). The effect is related to the changes of the ratio of molecule travelling time to residence time in the adsorbed state, as well as a strong influence of surface saturation by the absorbed molecules on the tangential momentum accommodation coefficient, which is supported by the derived model. Synergetic contribution of these two factors allows to enhance the separation factor of permanent and condensable gases strongly beyond the Knudsen limit, while maintaining a high permeance of porous membranes.

1. Introduction

Selective gas transport in membrane materials is commonly associated with two general factors: sorption and diffusion of molecules through specific binding sites or structural fragments. Dissolution of gas molecules in the membrane material plays a crucial role on the permeance of rubbery polymeric membranes [1]. However, for rigid glassy polymeric materials [2] and inorganic membranes, this factor is commonly omitted being superseded by the diffusion rates [3]. However, for inorganic membranes, the diffusion rates are still strongly affected by the interaction of penetrants with the surface. Two special cases can be considered here depending on the ratio of molecule travelling to residence times: small lengthscale of the diffusive jump (hopping or configurational diffusion, characteristic for microporous materials) and large jump lengths (Knudsen diffusion, characteristic for mesoporous solids) [4,5]. The latter case is known to provide very high permeance of membranes but very low selectivity, governed by molecules velocity, which is inversely proportional to the square root of the molecular mass [6]. Low Knudsen selectivity strongly limits technological utilisation of porous membranes. On the other hand, the control of gas-wall interaction, adjusting the ratio of molecule travelling time to the time of residence in the absorbed state, seems to be a prospective way for increasing the separation factor beyond the Knudsen limit.

Currently little attention is paid to this way of improving membrane performance. Despite modification of mesoporous membranes being proposed for controlling gas-wall interaction [7] or surface flow of adsorbed species [8], there has been no consideration given to the role of diffusion jump length on membrane selectivity.

Typically, organosilane compounds such as chlorosilanes or alkoxysilanes are utilized for the modification of porous ceramic or Vycor porous glass membranes. Polycondensation of functional groups of modifiers, with surface hydroxyl groups, leads to the linking of organosilane molecules with the membrane surface by covalent bonds and the formation of a grafted molecular monolayer. The chemical nature, and the length of alkyl chain, of the modifier molecules have a strong influence on the properties of the modified membranes. For example, modification of porous Vycor membranes, with an average pore diameter of 4 nm, with long chain alkylchlorosilanes leads to the increased adsorption of hydrocarbons. This, in turn, leads to a huge increase of membrane selectivity [9–11]. The same effect was observed for CO_2 adsorption in grafted fluorosilane layers, leading to enhanced CO_2 transport through modified ceramic and glass membranes [12,13]. The effect of specific interaction of the modifier functional group with gas molecules can be also utilized for increasing membrane selectivity.

* Corresponding author at: Department of Chemistry, Lomonosov Moscow State University, 1-3 Leninskiye gory, Moscow 11 9991, Russia.
E-mail address: di.petukhov@gmail.com (D.I. Petukhov).

https://doi.org/10.1016/j.seppur.2019.03.078
Received 31 July 2018; Received in revised form 13 March 2019; Accepted 25 March 2019
Available online 26 March 2019
1383-5866/

Typically, modification of the membrane surface with aminosilanes leads to an increase of membrane selectivity towards acidic gases, such as CO_2. The increase in carbon dioxide transport rate was explained previously, by the reaction of CO_2 with surface amine groups leading to the formation of carbamate species and surface "hopping" of carbon dioxide [14–19].

Surface modification of mesoporous solids by organosilanes has been used to control gas-solid interaction in Knudsen or transitional flow regime by B. Besser and co-authors [7,20,21]. The correlation between the kinetic diameter of gas molecules and permeance reduction in surface-modified YSZ (Yttria-stabilized zirconia) membranes has been investigated. Authors attributed enhanced CO_2/N_2 selectivity to surface diffusion and have suggested that immobilized alkyl chains limit the adsorption-desorption direction of molecules colliding with the pore wall. This leads to an increase in the diffusion path with a corresponding reduction of the membrane permeance. However, the authors didn't consider the role of residence times on the separation efficiency and attributed the observed effects to surface diffusion and steric effects. The same effect has been previously proposed theoretically by Krishna [22]

Notably, all the earlier studies on examining the effect of gas-wall interactions on transport characteristics of surface functionalized nanoporous membranes, were carried out using porous systems with irregular porosity, which strongly limits quantitative assessment of the collision frequency. Meanwhile, current progress in membrane technology enables easy design and manufacture of anodic aluminum oxide (AAO) membranes with strictly defined pore diameters and regular through porosity. Thus, this current study used AAO membranes, with pore diameters ranging from 10 to 100 nm, for evaluating the role of gas-wall interactions and diffusion jump lengths on gaseous diffusion rates in surface-functionalized nanochannels. In this pore diameter range, Knudsen diffusion is usually dominant amongst other gas transport mechanisms.

To attain maximal grafting density on the alumina surface, alkylphosphonic acid was utilized rather than organosilanes, which are normally used for modifying silica surfaces [23]. The phosphoryl group of organophosphonic acids is effectively bound with Lewis acid sites on alumina surface, resulting in the anchoring of modifier molecules. Previously, alkylphosphonic acid (n-dodecylphosphate) was used for surface modification of ceramic membranes resulting in a strong enhancement of propane/nitrogen selectivity coefficient due to the blocking of pore necks with alkyl chains [24].

2. Experimental

2.1. Membrane preparation

Anodic alumina membranes were prepared using conventional procedures described elsewhere [25,26]. After surface pretreatment, by electropolishing, metallic aluminum was anodized in a two-electrode cell in 0.3 M $H_2C_2O_4$ at a voltage range from 10 to 120 V. To obtain a hierarchical structure, with the macroporous layer branching into selective layer, the anodization voltage was gradually reduced from 40 V to 10 V. The thickness of membranes (or thickness of supporting and selective layers) was controlled by the total electric charge passed during anodization. After anodization, membranes with open through porosity were prepared by selective dissolution, of any remaining aluminum, in copper chloride (0.5 M $CuCl_2$ dissolved in 5 vol% HCl) followed by chemical etching of the barrier layer in 3 M H_3PO_4 aqueous solution with electrochemical detection of pore opening [27].

2.2. Membrane modification

A saturated solution of octadecylphosphonic acid $C_{18}H_{37}PO_3H_2$ (ODPA, Aldrich, 97%) in ethanol with a concentration of ~2.3 mM was used for membrane modification [28]. To avoid fouling, with undissolved ODPA, the solution was prefiltered through Chromafil Xtra 0.2 μm filter. For membrane modification, prefiltered solution of ODPA in ethanol was passed through an anodic alumina membrane placed in a dead-end Teflon filtration cell, under a transmembrane pressure equal to 2 bar [29]. The total volume of passed solution was equal to 5 ml per membrane area of 0.5 cm^2. After modification, membranes were washed twice by passing 5 ml of pure ethanol and then dried at 60 °C in argon atmosphere.

2.3. Membrane characterization

Scanning electron microscopy (SEM) images were recorded using a Leo Supra 50VP instrument. Determination of pore size distribution and membrane porosity was performed by statistical analysis of SEM images using ImageJ software. Fourier transformed infrared spectroscopy studies were performed using a Spectrum One spectrometer (Perkin Elmer) in range 500–4000 cm^{-1}. All spectra were acquired in the transmission geometry. Raman spectroscopy studies were performed on a Renishaw InVia spectrometer using He-Ne laser excitation (633 nm). Thermal analysis with EGA-MS was performed, using STA 209 PC Luxx instrument equipped with QMS 403 Aeolos mass spectrometer (Netzch, Germany), in air by heating to 1200 °C at 5 °C/min heating rate.

Gas permeance of the membranes was measured using two schemes – a differential scheme, described earlier in [5], for membranes with a permeance higher than 1 $m^3/(m^2 \cdot bar \cdot h)$ and an integral scheme, described earlier in [30], for membranes with a permeance lower than 1 $m^3/(m^2 \cdot bar \cdot h)$. In the case of the differential scheme, gas flux through the membranes was measured by mass-flow controllers Brooks SLA 5850 and the pressure difference on the membrane was measured by Carel SPKT00E3R pressure transducers. In the integral scheme measurements, a pressure growth rate, in the preliminary vacuumed permeate chamber of calibrated volume, was registered. The measurements performed for the same membrane using different schemes showed identical results.

Mixed gas permeation experiments for binary CH_4/C_4H_{10} mixtures were performed using both normal and isobutane. The methane concentration in the feed stream was 90 vol%. The upstream side of the membrane was in contact with a steady state flow of feed mixture at 1 bar, while the downstream side was swept by a carrier gas (He). The concentrations of methane and butane in the sweep stream and in the feed stream were determined using a Clarus 600 (Perkin Elmer) gas chromatograph equipped with a thermal conductivity detector.

3. Results and discussions

An accurate determination of porosity and average pore diameter was performed by statistical analysis of SEM images of both top and bottom surfaces of the membranes. The obtained SEM images and relevant pore size distributions are shown in Fig. 1. Average pore diameter and AAO membranes porosity are listed in Table 1. For the asymmetrical membrane AAO-40-10, the parameters of selective layer formed at 10 V are given.

Gas permeance characteristics of pristine membranes were measured for both non-condensable (He, N_2, CH_4) and condensable gases (C_2H_6, C_3H_8, n–C_4H_{10}, i-C_4H_{10}). An analysis of the membrane's permeance was performed using the protocol reported earlier in Ref [5]. The dependences of membrane permeance *vs.* Knudsen number, were fitted by a combination of Knudsen diffusion and viscous flow. Knudsen numbers for all experimental conditions were calculated using upstream and downstream pressures, gas characteristics (viscosity and molecular weight) and membrane average pore diameter:

$$K_n = \frac{\lambda}{d} = \frac{\eta}{\bar{P} d}\sqrt{\frac{\pi RT}{2M_r}} \quad (1)$$

where η – gas viscosity, d – average pore diameter, $\bar{P}$ – average

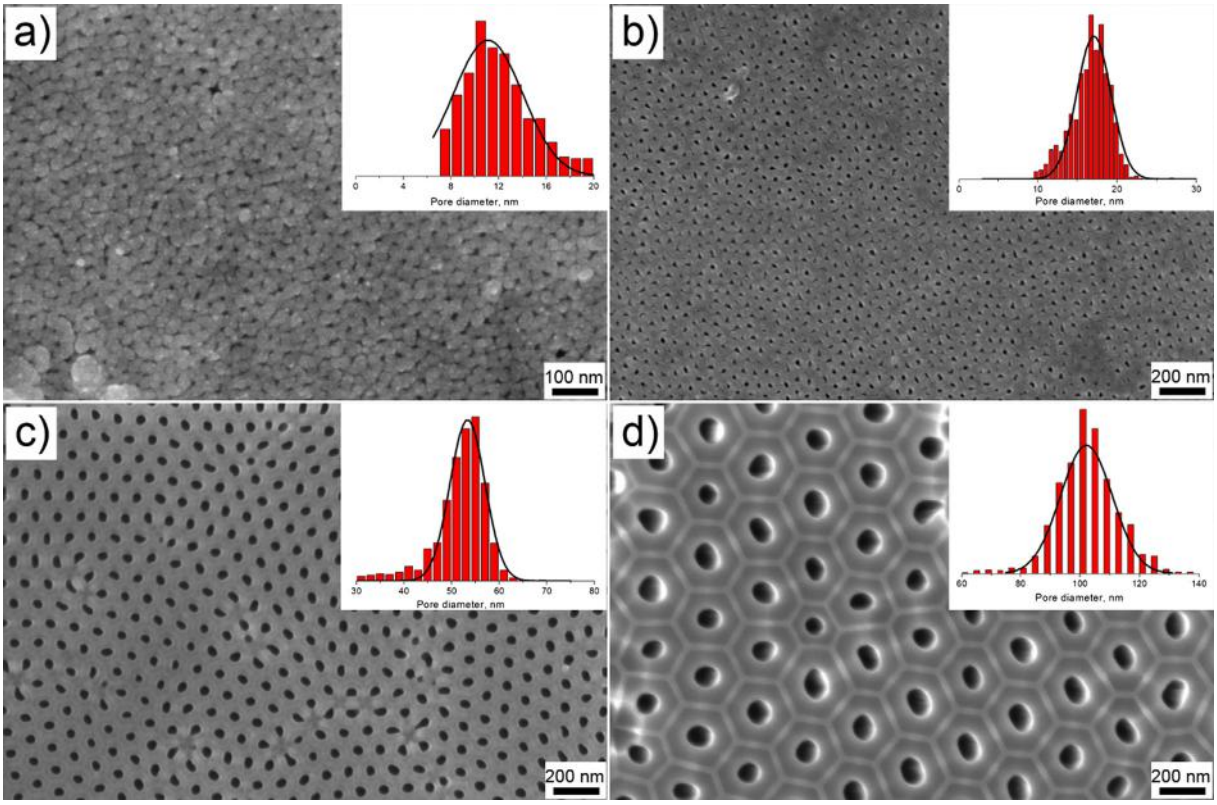

Fig. 1. Microstructure and pore size distribution of the studied membranes: (a) AAO-40-10, (b) AAO-20, (c) AAO-40, (d) AAO-120.

pressure, calculated as a half-sum of the feed and the permeate pressure, M_r – gas molecular weight.

Typical dependencies of membrane permeance, multiplied by the square root from the gas molecular weight vs. Knudsen number, are plotted in Fig. 2. In these coordinates the normalized permeances for all gases should degenerate into a single dependence on Knudsen numbers if no additional flow contributions occur. Obtained results were fitted using the following equation:

$$F\cdot\sqrt{M_r} = F_{Kn}\cdot\sqrt{M_r}\cdot\left(1+\frac{3\pi}{128\cdot K_n}\right) = A_{gas}\cdot\left(1+\frac{3\pi}{128\cdot K_n}\right), \quad (2)$$

where $F_{Kn}=\frac{\varepsilon d}{3RTL}\sqrt{\frac{8RT}{\pi M_r}}$ – membrane permeance in Knudsen diffusion regime and K_n – Knudsen number. This equation considers additive contributions of viscous flow $\left(\frac{3\pi}{128\cdot K_n}\text{ term}\right)$ and diffusive molecular fluxes (A_{gas} coefficient). The fitted values of A_{gas},for different gases and membranes, are listed in Table 1. It can be seen that the obtained coefficients decrease with increasing gas collision diameter, as was mentioned earlier in [5]. One can see that the data for different gases closely arrange into a single dependence for the AAO-120 membrane, while they separate in a series for AAO-40-10. Such behavior has been attributed to self-diffusion of penetrant gases due to intermolecular collisions, or slip enhancement due to tangential momentum accommodation growth with decreasing molecule's effective collision area. Thus, the gas permeance of pristine anodic alumina membranes can be described as a combination of viscous and diffusive fluxes, with a contribution of slip flow enhancement due to tangential momentum accommodation coefficient changes. The contribution becomes more pronounced with decreasing pore diameters, down to several nanometers. A strong increase in membrane permeance for n- and isobutane at low K_n values for AAO-40-10 membrane, can be explained by a capillary condensation effect, discussed in detail in [31,32].

Further modification of membranes with a highly flexible surface layer of octadecyl chains was performed to reveal the effect of gas-wall interactions and residence times on the separation performance. To confirm grafting of octadecylphosphonic acid at the membrane's modification stage, IR- and Raman spectroscopy studies were carried out. Fig. 3a shows the FT-IR spectra of initial and modified membranes. The presence of C-H stretching modes can be clearly seen in the spectra of the modified membrane. Peaks at wavenumbers 2961, 2924 and 2853 cm^{-1} correspond to symmetric valence vibration of CH_3- and -CH_2- groups, and asymmetrical valence vibration of -CH_2- group in octadecyl chain, respectively [33]. At the same time, FT-IR spectroscopy, in transmission geometry, didn't provide information on the distribution of the modifier agent over the membrane thickness. Thus, confocal Raman spectroscopy was applied to acquire spectra from the top and the bottom surfaces of the membranes (Fig. 3b,c). No

Table 1
Microstructural parameter and normalized gas permeance for pristine membranes.

Membrane	Pore diameter, nm	Porosity, %	Normalized gas permeance (A), $m^3\cdot kg^{0.5}/(m^2\cdot bar\cdot h\cdot mol^{0.5})$						
			He	N_2	CH_4	C_2H_6	C_3H_8	n-C_4H_{10}	i-C_4H_{10}
AAO-40-10	11 ± 3	7	2.82	2.55	2.41	2.37	2.32	2.26	2.29
AAO-20	16 ± 3	10	2.35	2.04	1.93	1.89	1.83	1.75	1.78
AAO-40	54 ± 5	22	7.2	7.05	6.68	6.50	6.20	5.89	5.99
AAO-120	102 ± 9	13	9.20	8.51	8.31	8.03	8.39	8.29	8.21

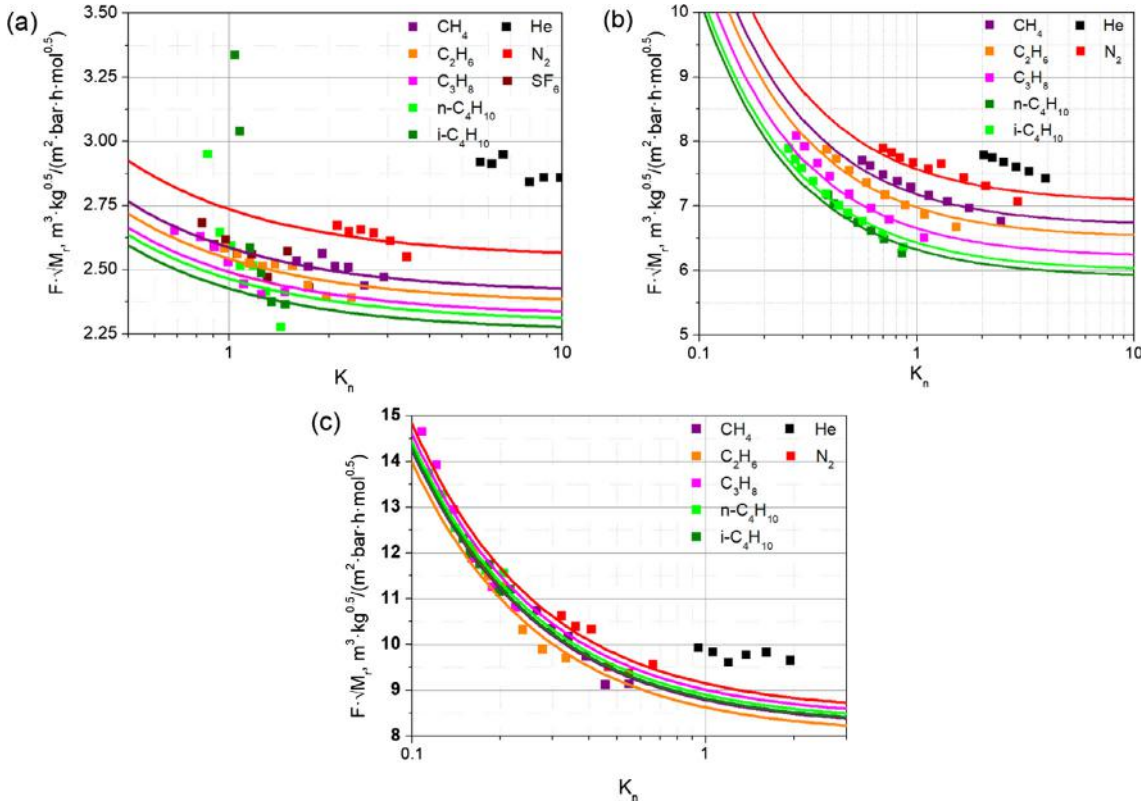

Fig. 2. Dependence of membrane permeance multiplied by the square root of penetrant molecule weight *vs.* Knudsen number for initial AAO-40-10 (a), AAO-40 (b) and AAO-120 (c) membranes.

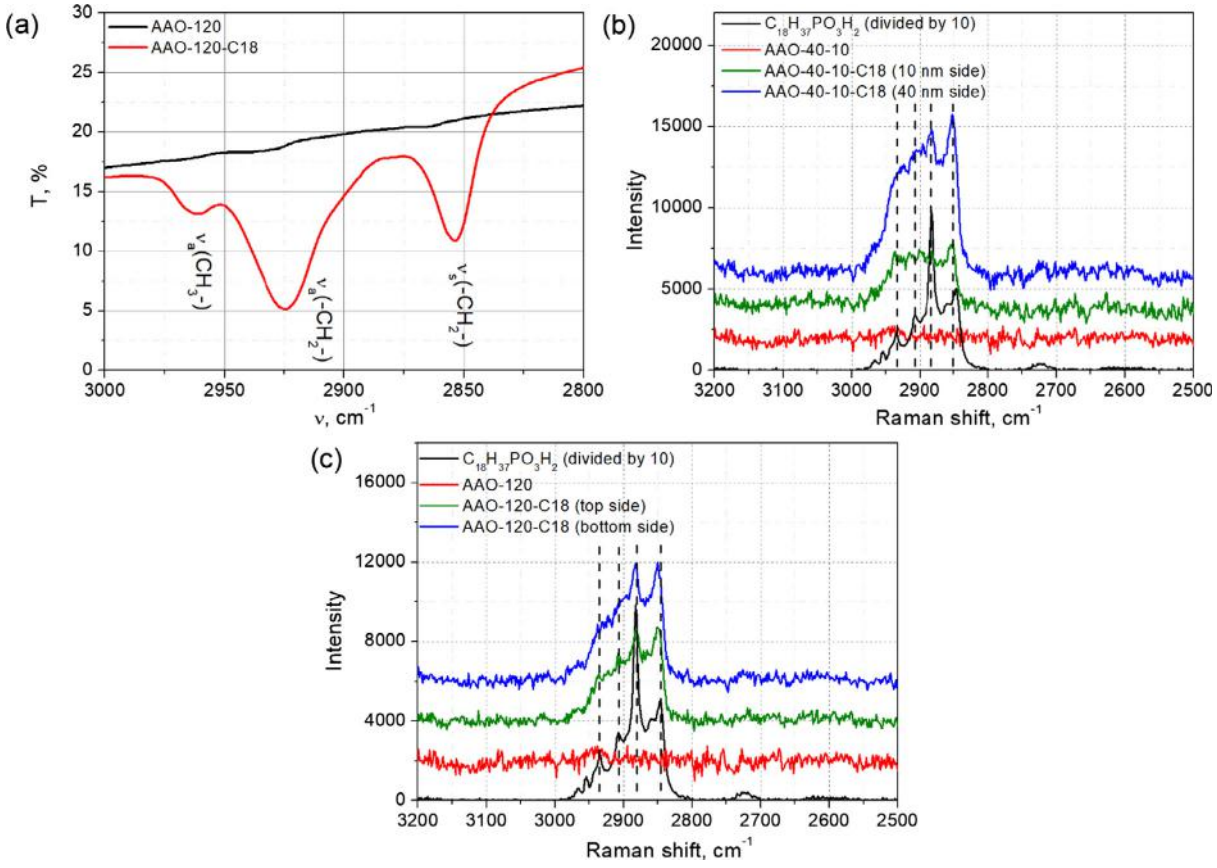

Fig. 3. IR spectra for initial and modified AAO-120 membrane (a). Raman spectra of initial and modified AAO-40-10 (b) and AAO-120 (c) membranes.

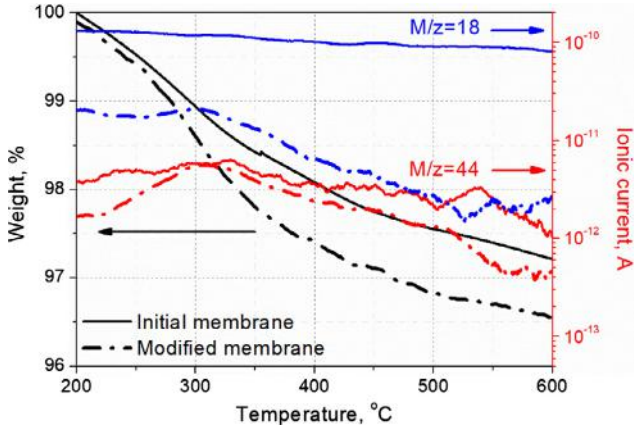

Fig. 4. Thermal analysis results and MS-signal for mass number 44 (CO_2) and 18 (H_2O) for initial and modified membranes.

characteristic ν(C-H) vibrations were observed for the pristine membranes, while well-defined peaks at 2924 cm^{-1}, 2852 cm^{-1}, 2882 cm^{-1} and 2908 cm^{-1} corresponding to symmetric -CH_2- and asymmetric -CH_2- and -CH_2-P valence vibrations, appear in the spectra of modified membranes. Raman signal intensities, from the top and bottom sides of membranes, are very similar in the case of the AAO-120-C18 sample but vary for the AAO-40-10-C18 membrane. This suggests some inhomogeneity in depthward distribution of octadecylphosphonic acid in membranes with low diameter pores (side of membrane with 10 nm pore diameter was positioned to the feed volume of modifier solution during modification stage). However, a strong difference in active surface area of membrane sides having 10- and 40 nm pores is noticeable, which can explain the difference in scattering intensity by the quantity of modifier agent grafted to the surface. In every instance, Raman spectroscopy confirms an in-depth modification of AAO surface by octadecylphosphonic acid.

To evaluate the quantity of immobilized octadecylphosphonic acid a thermal analysis of the modified sample was performed using EGA-MS. Fig. 4 shows the relative weight loss and ionic currents for mass numbers 18 (H_2O) and 44 (CO_2) in the evolved gases for initial and modified membranes. The difference in weight loss between the initial and modified membrane appears from ~220 to 550 °C, being accompanied by H_2O and CO_2 evolution. This temperature range corresponds well to the decomposition of immobilized alkyl chains, allowing an estimation of the grafting density from the weight loss difference. Taking into account the specific surface area of anodic alumina of 9.1 m^2/g [31] and the difference in weight loss of 0.62%, one can calculate an alkyl-chain density of 1.6 molecules per nm^2. The value is substantially smaller when compared to the areal density for OH-groups on alumina of 5–8 nm^{-2} [34]. Nevertheless, the obtained value is considered high enough to have an influence on gas-wall interactions and gas accommodation coefficients due to specific adsorption of molecules in the grafted layer.

Gas permeance of modified membranes was studied and processed in the same manner to the initial membranes (Fig. 5). The permeance for all the membranes generally decreased upon modification. However, the permeance reduction coefficient was found to depend strongly on the gas nature and channel diameter. On Fig. 6 the permeance loss factors for different gases, normalized to the permeance loss factor for helium, are plotted for modified nanoporous membranes. Helium was utilized as a reference gas as it provides minimal interaction between gas molecules and grafted compounds. The divergence of the permeance reduction, for different gases, increases with diminishing pore diameter. Moreover, for the membranes with minimal channel diameters (AAO-40-10-C18 and AAO-20-C18), the permeance of permanent gases falls to very low values of 0.03–0.1 $m^3/(m^2 \cdot bar \cdot h)$.

A direct mathematical description of the experimental data for modified membranes, using Eq. (2), could not be calculated due to an inequivalent growth of the dependences for permanent and condensable gases. Hence, an additional independent parameter, accounting for different K_n dependence for different gases has been introduced:

$$F \cdot \sqrt{M_r} = A_{gas} \cdot \left(1 + \frac{B_{gas}}{K_n}\right) \tag{3}$$

The fit was performed using the same ratio of A_{gas} parameters to pristine membranes. Fitting results for AAO-40-C18 and AAO-120-C18 membranes are listed in Table 2.

According to the fitted results, experimental permeances for the AAO-120-C18 membrane are reasonably described by a simple combination of viscous flow and Knudsen diffusion with the B_{gas} parameter close to 3π/128 for all gases. This is explained by the large diameter of the pores (~100 nm) exceeding the mean free path of penetrant molecules. However, for the AAO-40-C18 membrane, an enhancement of transport for hydrocarbons is clearly seen, which is due to increasing B_{gas} coefficients with gas molecular weight and decreasing of saturation pressure. To quantify the additional contribution, the difference between experimental permeance values and the values predicted by Eq. (2) (Knudsen and viscous flow), was analyzed. The A_{gas} parameters used in the calculations were extracted from fitting of experimental data with Eq. (3). The resulting maximal values for this contribution (at lowest K_n) for AAO-40-C18 membrane, equal 9% for CH_4, 11% for C_2H_6, 25% for C_3H_8, 43% and 34% for n- and isobutane, respectively.

Typically, such contributions are associated with surface flow of adsorbed molecules in the grafted layer. Thus, we attempted to evaluate the maximal value of surface flux, considering the flow of liquid condensate in the grafted layer with a thickness of 2 nm and using the pressure difference of feed and permeate sides taking into account Poiseuille flow in a plane layer, was carried out:

$$F_{surf} = \frac{\varepsilon \xi^3 \rho V_m}{3\eta_{cond.} L d M_r} \tag{4}$$

where ε- membrane porosity, ζ – the thickness of adsorbate layer, ρ – condensate density, $\eta_{cond.}$ – condensate viscosity, L – membrane thickness.

The upper-bound estimation of surface flux for n-butane gives ~0.2%, which is negligible compared to the experimental results. Thus, surface diffusion can't explain the huge enhancement of hydrocarbons transport at low Knudsen numbers.

Substantial decrease of the permeance for modified membranes and the relative increase of hydrocarbons transport can be either explained by an increase of the molecules residence time at the surface, or by increasing the flight path due to a narrowing of the desorption angle distribution as suggested earlier in [7]. Neither of the reasons can be unambiguously preferred, at the current stage, due to the lack of experimental data. Further studies with different modifier chain lengths or permeance temperature dependences could help to resolve the issue. Nevertheless, an attempt to describe experimental results with a model, considering timing parameters only and without taking into account the changes of the desorption angles total flight path due to strong difficulties of including those parameters into mathematical formulation, can be made.

To describe permeance changes with surface modification, one can suggest a decrease of desorption constants shifting an equilibrium of free ($[S_{free}]$), and occupied ($[S_{ad}]$), sites at the surface with corresponding of increase of surface residence time:

$$\frac{[S_{ad}]}{[S_{free}]} = \frac{k_{ads}}{k_{des}} \frac{P_{gas}}{P_0} = k_{gas} \frac{P_{gas}}{P_0}, \tau_{res} = \frac{1}{k_{des}[S_{ad}]} \tag{5}$$

where k_{ads} and k_{des} denote reaction constant for adsorption and desorption processes, respectively, P_{gas} – is the absolute gas pressure, P_0 – is the gas saturation pressure and τ_{res} corresponds to an average molecular

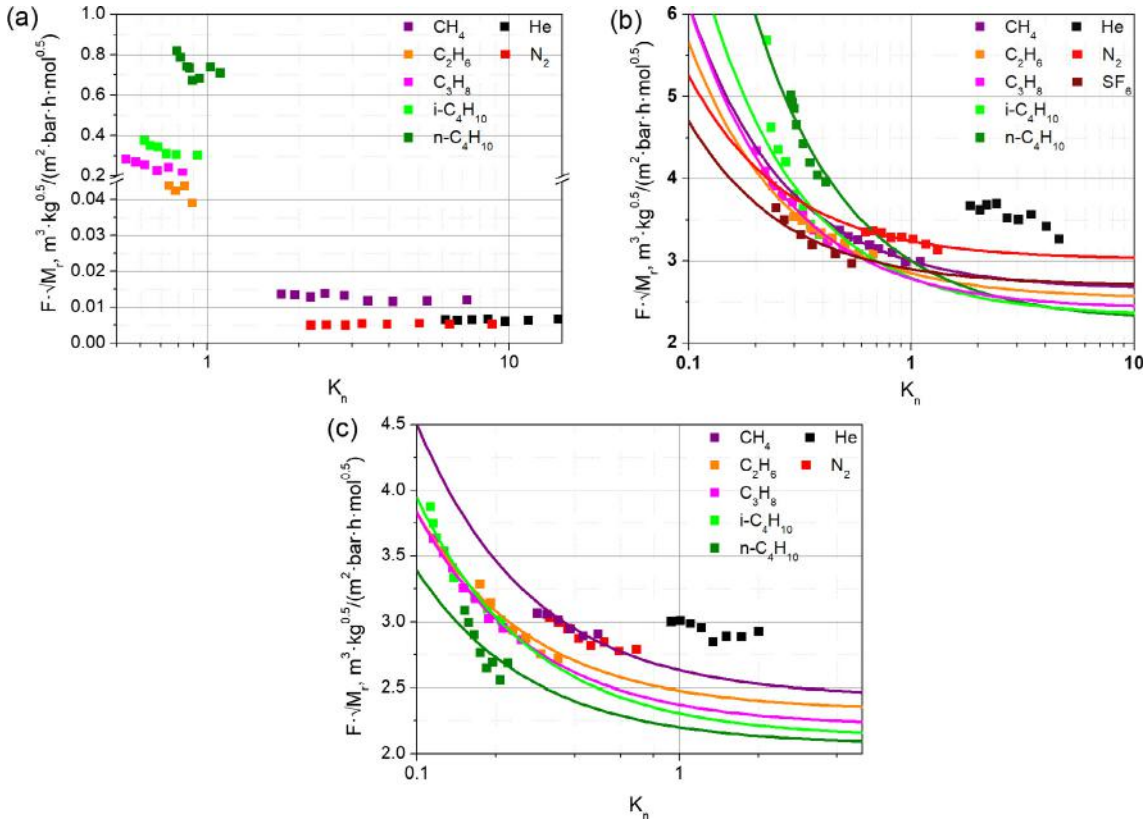

Fig. 5. Dependence of membrane permeance multiplied by square root of penetrant molecule weight vs Knudsen number for modified AAO-40-10-C18 (a), AAO-40-C18 (b) and AAO-120-C18 (c) membranes.

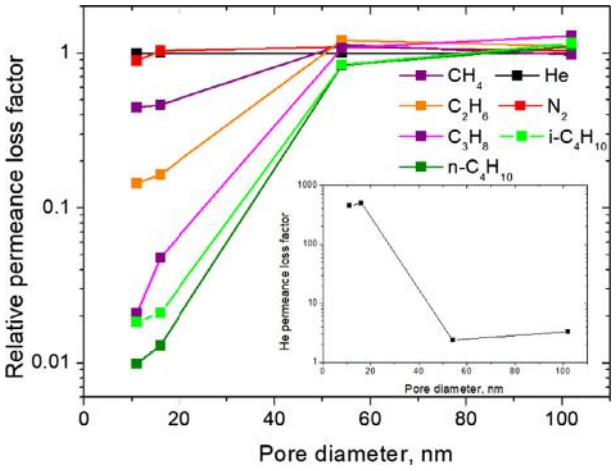

Fig. 6. Permeance loss factors of different gases normalized to permeance loss of helium for modified nanoporous membranes, depending on the pore diameter.

residence time in the adsorbed state on the pore wall.

The gas flux through the membrane can be formulated as the number of molecules inside pore (N_{molec}) divided by an average in-pore retention time for the molecule ($t_{in\text{-}pore}$):

$$F \sim \frac{N_{molec}}{t_{in\text{-}pore}} \tag{6}$$

The total duration a molecule spends in the pore can be considered as a sum of average molecular free flight time (τ_{fly}) and residence time in the adsorbed state on the pore wall (τ_{res}) multiplied by the number of gas-wall collisions (N_{col}):

$$t_{inpore} = N_{col}(\Pi_{ads}\cdot\tau_{res} + \tau_{fly}),\ \tau_{fly} = d\sqrt{\frac{\pi M}{8RT}} \tag{7}$$

where Π_{ads} represents the probability of molecule adsorption by a free surface site and τ_{fly} is found by division of an average pore diameter by the average thermal speed of the molecules.

Obviously, an effective absorption of condensable gases, with low saturation pressure, results in high surface coverage (θ) and substantial reduction of the available surface. Collision of gas molecules with the absorbed surface layer, at high saturation, should result in molecular reflection without loss of tangential momentum. Thus, the term Π_{ads} ,describing the probability of molecule adsorption by a free surface site or specular reflection by an occupied site, has been introduced into Eq. (6). If an equal number of collisions and equal total traveling distance of molecules, in pristine and modified membrane, is now assumed, the relation between their gas permeances as an inverse ratio of the total duration molecules spend in the pore for pristine and modified membranes can be written:

$$\frac{F}{F_0} = \frac{t_{inpore,0}}{t_{inpore}} = \frac{\Pi_{ads,0}\cdot\tau_{res,0} + \tau_{fly}}{\Pi_{ads}\cdot\tau_{res} + \tau_{fly}} \tag{8}$$

Furthermore, assuming negligible residence time for pristine membrane ($\tau_{res,0}$) the expression can be simplified to:

$$\frac{F}{F_0} \approx \frac{\tau_{fly}}{\Pi_{ads}\cdot\tau_{res} + \tau_{fly}} \tag{9}$$

Fractional occupancy of the adsorption sites is easily introduced, with Langmuir adsorption isotherm, with the probability of molecule adsorption calculated as:

$$\Pi_{ads} = 1 - \theta = 1 - \frac{k_{gas}\frac{P_{gas}}{P_0}}{1 + k_{gas}\frac{P_{gas}}{P_0}} = \frac{1}{1 + k_{gas}\frac{P_{gas}}{P_0}} \tag{10}$$

Table 2
Fitting parameters for modified AAO-40-C18, AAO-120-C18 membranes.

Gas	Membrane						Condensation pressure (P_0), bar at T = 25 °C
	AAO-40-C18			AAO-120-C18			
	A	B	Contribution of additional flow at P_{feed} = 2 bar, %	A	B	Contribution of additional flow at P_{feed} = 2 bar, %	
N_2	3.01	0.074	–	2.46	0.074	–	–
CH_4	2.65	0.131	4.4	2.43	0.086	1.1%	–
C_2H_6	2.54	0.122	8.4	2.33	0.065	–	41.8
C_3H_8	2.41	0.153	12.8	2.21	0.073	–	9.53
i-C_4H_{10}	2.32	0.205	21.8	2.12	0.086	2.3%	3.51
n-C_4H_{10}	2.26	0.328	37.2	2.07	0.064	–	2.43

Using (10), Eq. (9) can be rewritten in the following manner:

$$\frac{F}{F_0} = 1 - \frac{\tau_{res}}{\tau_{res} + \tau_{fly}\left(1 + k_{gas}\frac{P_{gas}}{P_0}\right)} \tag{11}$$

The provided model describes the decrease of the permeance of membranes proportional to the characteristic ratio of molecule travelling and residence times. The flight times are governed by gas velocities and the diameter of the pores, while residence times, in the absorbed state, are obviously dependent on the chemical nature of the penetrant molecules and the modifier agent. Generally, the tendencies defined by Eq. (11) are well supported by the experimental results. Moreover, due to strong interaction of hydrocarbons with alkyl chains, significant surface coverage in modified membranes, by C_1-C_4 hydrocarbons, can be expected. Thus, further analysis of the tangential momentum accommodation coefficient (TMAC), corresponding to the fraction of the specular reflections during molecular-wall collisions has been conducted. TMAC values (α) were extracted from experimental data in terms of slip flow using Eq. (19) from Ref. [5]. This equation corresponds to the combination of Knudsen diffusion and viscous flow (similar to Eq. (2)) and involves an additional term, accounting for the contribution of specular reflections of gas molecules from the pore walls:

$$F_{Slip} = F_{Kn}\left(\frac{3\pi}{128\cdot K_n} + \frac{3\pi}{64} + \frac{3\pi}{8\sqrt{2}}\cdot\frac{2-\alpha}{\alpha}\right) \approx F_{Kn}\left(1 + \frac{3\pi}{128\cdot K_n} + \frac{3\pi}{8\sqrt{2}}\cdot\frac{2-2\alpha}{\alpha}\right) \tag{12}$$

$$\alpha = \frac{2}{\frac{F_{add}}{F_{Kn}}\cdot\frac{8\sqrt{2}}{3\pi} + 2} \tag{13}$$

A strong correlation for TMAC values on the normalized pressure (P/P_0) for different gases has been obtained for the AAO-40-C18 sample, providing strong evidence of the proposed concept (Fig. 7). The fraction of specular reflections, increasing linearly with the reduced pressure, fits well with the Langmuir adsorption isotherm and the proposed Eq. (10).

For the membranes with smaller pore diameters (AAO-20-C18 and AAO-40-10-C18) the effects are enhanced several times. A drastic drop of permeance for non-condensable gases (300–400 times) and moderate decrease of the permeance of hydrocarbons (3.5–50 times) was observed (see Figs. 5 and 6). Despite these tendencies are principally described by the proposed model, absolute values are not fitted with unique timing parameters. Extracted residence times for helium vary from $\sim 5\cdot10^{-11}$ to $\sim 2\cdot10^{-9}$ s for membranes with different pore diameters. Large values of calculated residence time, obtained for membranes with minimal channel diameters, can be associated with possible blocking of pore necks by the overlapping alkyl chains of modifier molecules. Notably, the length of the octadecyl tail is 1.6 nm which gives a total modifier layer thickness of ~2 nm. This value is strongly below the radius of the pores of AAO-40-10 and AAO-20 membranes.

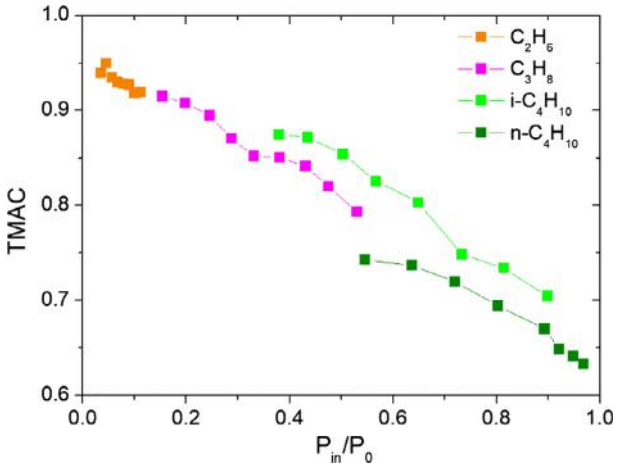

Fig. 7. The dependence of calculated TMAC values on normalized feed pressure for modified AAO-40-C18 membrane for different hydrocarbons.

However, possible blocking of the channels is supported by an increase of O_2/N_2 selectivity to the factor of 2. Nevertheless, an appearance of such necks in the channels has much less effect on the permeance of hydrocarbons, having large solubility and diffusivity in paraffins, which still allows an analysis of their permeance with the proposed model. The utmost values of hydrocarbon TMACs, extracted using the model, increase with decreasing pore diameters from ~1 for membranes with 100 nm pores to values below 0.5 for membranes with 10 nm pores. Despite providing some predictive power for permeance of surface modified membranes quantitative assessment of the model is still required. Further data acquisition, and analysis for membranes with small pore diameters, is necessary to provide a full theoretical description.

According to the proposed model, the maximum effect of surface modification can be attained at low pore diameters using modifier agents providing large residence times. Moreover, an additional enhancement of membrane selectivity, for condensable gases, can be acquired by an increased quantity of specular reflection and slip flow of penetrant. Synergetic contribution of these two factors allows to obtain membrane with ideal selectivity for n-butane/methane pair up to 32, with butane permeance of 3 $m^3/(m^2\cdot bar\cdot h)$ (Table 3), exceeding the Knudsen limit (0.52) by over 60 times. The selectivity for the i-C_4H_{10}/CH_4 pair is lower than for the n-C_4H_{10}/CH_4 pair due to the lower occupation density of isobutane molecules in the grafted layer, leading to a decreased number of specular reflections. The reported performance exceeds that reported for Vycor glass modified with octadecylchlorosilane [35].

Notably, the practical utilisation of membranes for separation of hydrocarbons mixtures implies mixed gas selectivity rather than ideal selectivity values. Mixed gas selectivity measurements of modified membranes for gas mixtures containing 90% of methane and 10% of n- or isobutane (Table 3) have been carried out. The mixed gas

Table 3
Pure- and mixed gas selectivity for n-C_4H_{10}/CH_4 и i-C_4H_{10}/CH_4 pairs for modified membranes.

Membrane	Minimal pores diameter in pristine membrane, nm	Selectivity			
		α(n-C_4H_{10}/CH_4)		α(i-C_4H_{10}/CH_4)	
		Pure gas	Mixed gas	Pure gas	Mixed gas
AAO-40-C18	54 ± 5	0.72	0.69	0.65	0.64
AAO-20-C18	16 ± 3	10.1	6.9	4.9	3.1
AAO-40-10-C18	11 ± 3	32.3	9.0	13.3	4.4

selectivities appear to be lower than ideal values for all the samples. This can be explained due to lower partial pressure of butane or isobutane leading to reduction of their transport efficiencies in comparison with the case of pure gases. However, the values obtained for the n-butane/methane mixed gas separation factor are higher than the same separation factors for PDMS membranes, which are widely used for hydrocarbon separation [36]. Moreover, immobilisation of grafted compounds on the rigid inorganic frameworks provides a solution to the problem of membrane degradation and selectivity losses. Thus, the suggested approach seems to be a prospective way for preparation of stable membranes for conditioning and processing of natural gases.

4. Conclusions

In summary, surface modification of nanoporous anodic alumina membranes with average pore diameter from 10 to 100 nm was successfully accomplished using octadecylphosphonic acid. Surface modification was proved by IR- and Raman spectroscopy. The results of thermal analysis, with EGA-MS, allowed the estimation of the grafting density of ~2 groups/nm^2. Single gas permeation measurements were performed for permanent (N_2, He, CH_4) and condensable gases (C_2H_6, C_3H_8, n-C_4H_{10}, i-C_4H_{10}). After modification, the permeance for all membranes generally decreased by over 3 times. In the case of membranes with average channel diameters below 50 nm, an additional contribution of hydrocarbons transport is clearly observed, which increases with a decrease of hydrocarbon saturation pressure. Decrease of pore diameters makes the effect more pronounced – for membranes with pore diameter lower than 20 nm, a drastic drop of the permeance for non-condensable gases (up to 400 times) and a moderate drop of hydrocarbon permeance (3.5–50 times) appears. The effect is explained by variation of the ratio of molecule travelling time and residence time in adsorbed state and strong influence of surface saturation by absorbed molecules on the tangential momentum accommodation coefficient, which is supported by suggested model. These effects allow lifting of the separation factor of permanent and condensable gases strongly beyond the Knudsen limit, while maintaining high permeance of porous membranes. Modified membranes. with 10-nm channel diameters, possess 32.3 and 9.0 ideal and mixed gas separation factors for n-C_4H_{10}/CH_4 pair with n-C_4H_{10} permeance up to 3.5 $m^3/(m^2 \cdot bar \cdot h)$. Thus, surface modification of nanoporous membranes can be considered as a prospective way for the preparation of stable membranes for efficient separation of hydrocarbons.

Acknowledgments

The work is supported by the Ministry of Science and Higher Education of the Russian Federation within a Federal Targeted Programme for “Research and Development in Priority Areas of Development of the Russian Scientific and Technological Complex for 2014 – 2020” (Agreement No. 14.604.21.0177, unique Project Identification RFMEFI60417X0177).

References

[1] Y. Yampolskii, Polymeric Gas Separation Membranes, Macromolecules 45 (2012) 3298–3311, https://doi.org/10.1021/ma300213b.
[2] A. Alentiev, Y. Yampolskii, V. Ryzhikh, D. Tsarev, The database “Gas Separation Properties of Glassy Polymers” (Topchiev Institute): capabilities and prospects, Pet. Chem. 53 (2013) 554–558, https://doi.org/10.1134/S0965544113080033.
[3] S. Thomas, R. Schafer, J. Caro, A. Seidel-Morgenstern, Investigation of mass transfer through inorganic membranes with several layers, Catal. Today. 67 (2001) 205–216, https://doi.org/10.1016/S0920-5861(01)00288-7.
[4] A.B. Shelekhin, A.G. Dixon, Y.H. Ma, Theory of gas diffusion and permeation in inorganic molecular-sieve membranes, AIChE J. 41 (2018) 58–67, https://doi.org/10.1002/aic.690410107.
[5] D.I. Petukhov, A.A. Eliseev, Gas permeation through nanoporous membranes in the transitional flow region, Nanotechnology 27 (2016) 085707, , https://doi.org/10.1088/0957-4484/27/8/085707.
[6] G.M. Fryer, A theory of gas flow through capillary tubes, Proc. R. Soc. Lond. A. Math. Phys. Sci. 293 (1966) 329–341 http://www.jstor.org/stable/2415472.
[7] B. Besser, S. Malik, M. Baune, S. Kroll, J. Thöming, K. Rezwan, The influence of the functional group density on gas flow and selectivity: nanoscale interactions in alkyl-functionalized mesoporous membranes, Microporous Mesoporous Mater. 237 (2017) 38–48, https://doi.org/10.1016/j.micromeso.2016.09.026.
[8] R.J.R. Uhlhorn, K. Keizer, A.J. Burggraaf, Gas and surface-diffusion in modified gamma-alumina systems, J. Memb. Sci. 46 (1989) 225–241, https://doi.org/10.1016/S0376-7388(00)80337-3.
[9] A. Javaid, M.P. Hughey, V. Varutbangkul, D.M. Ford, Solubility-based gas separation with oligomer-modified inorganic membranes, J. Memb. Sci. 187 (2001) 141–150, https://doi.org/10.1016/S0376-7388(01)00341-6.
[10] K.C. McCarley, J.D. Way, Development of a model surface flow membrane by modification of porous γ-alumina with octadecyltrichlorosilane, Sep. Purif. Technol. 25 (2001) 195–210, https://doi.org/10.1016/S1383-5866(01)00103-4.
[11] R.P. Singh, J.D. Way, S.F. Dec, Silane modified inorganic membranes: effects of silane surface structure, J. Memb. Sci. 259 (2005) 34–46, https://doi.org/10.1016/j.memsci.2005.03.004.
[12] N. Abidi, A. Sivade, D. Bourret, A. Larbot, B. Boutevin, F. Guida-Pietrasanta, A. Ratsimihety, Surface modification of mesoporous membranes by fluoro-silane coupling reagent for CO2 separation, J. Memb. Sci. 270 (2006) 101–107, https://doi.org/10.1016/j.memsci.2005.06.054.
[13] R.P. Singh, J.D. Way, K.C. McCarley, Development of a model surface flow membrane by modification of porous vycor glass with a fluorosilane, Ind. Eng. Chem. Res. 43 (2004) 3033–3040, https://doi.org/10.1021/ie030679q.
[14] D. Stoltenberg, A. Seidel-Morgenstern, An attempt to alter the gas separation of mesoporous glass membranes by amine modification, Microporous Mesoporous Mater. 154 (2012) 148–152, https://doi.org/10.1016/j.micromeso.2011.11.013.
[15] D. Luebke, C. Myers, H. Pennline, Hybrid membranes for selective carbon dioxide separation from fuel gas, Energy Fuels 20 (2006) 1906–1913, https://doi.org/10.1021/ef060060b.
[16] M. Ostwal, R.P. Singh, S.F. Dec, M.T. Lusk, J.D. Way, 3-Aminopropyltriethoxysilane functionalized inorganic membranes for high temperature CO2/N2 separation, J. Memb. Sci. 369 (2011) 139–147, https://doi.org/10.1016/j.memsci.2010.11.053.
[17] S.B. Messaoud, A. Takagaki, T. Sugawara, R. Kikuchi, S.T. Oyama, Alkylamine–silica hybrid membranes for carbon dioxide/methane separation, J. Memb. Sci. 477 (2015) 161–171, https://doi.org/10.1016/j.memsci.2014.12.022.
[18] T. Takahashi, R. Tanimoto, T. Isobe, S. Matsushita, A. Nakajima, Surface modification of porous alumina filters for CO2 separation using silane coupling agents, J. Memb. Sci. 497 (2016) 216–220, https://doi.org/10.1016/j.memsci.2015.09.007.
[19] M. Ostwal, J.D. Way, Functionalized Inorganic Membranes for High-Temperature CO2/N-2 Separation, in: A.H. Lu, S. Dai (Eds.), POROUS Mater. Carbon dioxide capture, Springer, New York, 2014, pp. 223–245, , https://doi.org/10.1007/978-3-642-54646-4_7.
[20] B. Besser, T. Veltzke, J.A.H. Dreyer, J. Bartels, M. Baune, S. Kroll, J. Thöming, K. Rezwan, A comparative experimental study on the deviation of the ideal selectivity in HDTMS-functionalized and untreated ceramic structures with pores in the upper mesoporous range, Microporous Mesoporous Mater. 217 (2015) 253–261, https://doi.org/10.1016/j.micromeso.2015.06.042.
[21] B. Besser, A. Ahmed, M. Baune, S. Kroll, J. Thöming, K. Rezwan, Applying alkyl-chain surface functionalizations in mesoporous inorganic structures: their impact on gas flow and selectivity depending on temperature, ACS Appl. Mater. Interf. 8 (2016) 26938–26947, https://doi.org/10.1021/acsami.6b09174.
[22] R. Krishna, Investigating the validity of the knudsen diffusivity prescription for mesoporous and macroporous materials, Ind. Eng. Chem. Res. 55 (2016) 4749–4759, https://doi.org/10.1021/acs.iecr.6b00762.
[23] P.G. Mingalyov, G.V. Lisichkin, Chemical modification of oxide surfaces with organophosphorus(v) acids and their esters, Russian Chem. Rev. 75 (2006) 541–557.
[24] J. Randon, Preliminary studies on the potential for gas separation by mesoporous ceramic oxide membranes surface modified by alkyl phosphonic acids, J. Memb. Sci. 134 (1997) 219–223, https://doi.org/10.1016/S0376-7388(97)00110-5.
[25] D.I. Petukhov, K.S. Napolskii, A.A. Eliseev, Permeability of anodic alumina membranes with branched channels, Nanotechnology 23 (2012) 335601, , https://doi.org/10.1088/0957-4484/23/33/335601.
[26] D.I. Petukhov, K.S. Napolskii, M.V. Berekchiyan, A.G. Lebedev, A.A. Eliseev, Comparative study of structure and permeability of porous oxide films on aluminum obtained by single- and two-step anodization, ACS Appl. Mater. Interf. 5 (2013) 7819–7824, https://doi.org/10.1021/am401585q.

[27] E.S. Pyatkov, M.V. Berekchiyan, A.A. Yeliseyev, A.V. Lukashin, D.I. Petukhov, K.A. Solntsev, Electrochemical detection of barrier layer removal for preparation of anodic alumina membranes with high permeance and mechanical stability, Inorg. Mater. Appl. Res. 9 (2018) 82–87, https://doi.org/10.1134/S2075113318010227.
[28] M. Cichomski, K. Kośla, J. Grobelny, W. Kozłowski, W. Szmaja, Tribological and stability investigations of alkylphosphonic acids on alumina surface, Appl. Surf. Sci. 273 (2013) 570–577, https://doi.org/10.1016/j.apsusc.2013.02.081.
[29] D.I. Petukhov, D.A. Buldakov, A.A. Tishkin, A.V. Lukashin, A.A. Eliseev, Liquid permeation and chemical stability of anodic alumina membranes, Beilstein J. Nanotechnol. 8 (2017) 561–570, https://doi.org/10.3762/bjnano.8.60.
[30] E. Chernova, D. Petukhov, O. Boytsova, A. Alentiev, P. Budd, Y. Yampolskii, A. Eliseev, Enhanced gas separation factors of microporous polymer constrained in the channels of anodic alumina membranes, Sci. Rep. 6 (2016) 31183, https://doi.org/10.1038/srep31183.
[31] D.I. Petukhov, M.V. Berekchiian, E.S. Pyatkov, K.A. Solntsev, A.A. Eliseev, Experimental and theoretical study of enhanced vapor transport through nanochannels of anodic alumina membranes in a capillary condensation regime, J. Phys. Chem. C. 120 (2016) 10982–10990, https://doi.org/10.1021/acs.jpcc.6b02971.
[32] D.I. Petukhov, M.V. Berekchiian, A.A. Eliseev, Meniscus curvature effect on asymmetric mass-transport through nanochannels in capillary condensation regime, J. Phys. Chem. C. 122 (2018) 29537–29548, https://doi.org/10.1021/acs.jpcc.8b08289.
[33] R. Brambilla, G.P. Pires, J.H.Z. dos Santos, M.S.L. Miranda, B. Chornik, Octadecylsilane-modified silicas prepared by grafting and sol–gel methods, J. Electron Spectros. Relat. Phenomena. 156–158 (2007) 413–420, https://doi.org/10.1016/j.elspec.2006.12.053.
[34] V. Romero, V. Vega, J. García, R. Zierold, K. Nielsch, V.M. Prida, B. Hernando, J. Benavente, Changes in morphology and ionic transport induced by ALD SiO2 coating of nanoporous alumina membranes, ACS Appl. Mater. Interf. 5 (2013) 3556–3564, https://doi.org/10.1021/am400300r.
[35] K. Kuraoka, Y. Chujo, T. Yazawa, Hydrocarbon separation via porous glass membranes surface-modified using organosilane compounds, J. Memb. Sci. 182 (2001) 139–149, https://doi.org/10.1016/S0376-7388(00)00559-7.
[36] J. Schultz, K.-V. Peinemann, Membranes for separation of higher hydrocarbons from methane, J. Memb. Sci. 110 (1996) 37–45, https://doi.org/10.1016/0376-7388(95)00214-6.